Geo-Marine Letters (2020) 40:843–851
https://doi.org/10.1007/s00367-019-00594-y

ORIGINAL

Shallow sedimentation of Natal shelf and coastal erosion implications, NE Brazil

D. A. Moreira[1] · M. P. Gomes[1] · H. Vital[1]

Received: 29 March 2019 / Accepted: 4 September 2019 / Published online: 14 September 2019

Abstract
High-resolution seismic stratigraphic analysis to reconstruct the depositional history of the inner shelf Holocene successions was performed on the northeastern Brazilian, adjacent to Natal City. Boomer seismic data was collected between the coastline up to ~ 15-m water depth. Three seismic units and three seismic surfaces were observed with regional significance and low lateral variability. They represent the transgressive to highstand deposits lying on the Pleistocene/Holocene boundary surface S1—older, regional, and the irregular unconformity at ~ 35 m, forming a semi-enclosed environment near the coast. The basal unit (U1) is related to a moderate/high-energy environment and grade upward to units (U2 and U3) of lower energy conditions and thin thickness that decrease seaward with large through near coast on the west. Above this surface, chaotic and parallel internal configurations represent unit U1 that limited at the top by S2. The ravinement surface S2 at ~ 18 m reveals wave-tide influence in a very shallow inner shelf, which controlled the accommodation space and sediment transport. Unit U2 fills the scours with onlapping terminations over S2. The shallowest surface (S3) occurs at ~ 12 m below modern sea level probably associated with the maximum flooding surface underlying the U3 with dominant aggradation character in parallel/wavy configuration. U1 represents a shallow marine environment with a greater sediment supply controlled mainly by the water depth during the initial transgressive shelf inundation. The lower sediment accumulation of U2 and U3 indicates a decreasing of sediment supply, higher sediment transport or higher rates of erosion in shallow marine environments.

Introduction

Sedimentation in shallow shelf environments is generally related with the interaction between sediment supply, hydrodynamic regime (waves, tides, and currents), relative sea-level changes, coastal morphology, and rock resistance (Nittrouer et al. 2007; Campos and Dominguez 2010; Muehe 2010). Quaternary sea-level oscillations associated with climate change (Peltier 1998; Bezerra et al. 2003; Caldas et al. 2006; Bird et al. 2010; Lambeck et al. 2014) triggered erosion and sedimentation processes on coastal and shelf systems (D'Agostini et al. 2015; Cooper et al. 2018; Kalani et al. 2008; Menier et al. 2010). Sea level strongly affects the sedimentation of estuaries, bays, lagoon systems (Green et al. 2015; Benallack et al. 2016; Aleman et al. 2014; Aliotta et al. 2013), incised valleys (Menier et al. 2010; Lericolais et al. 2001; Tesson et al. 2015), and continental shelves (Edwards et al. 2003; Artusi and Figueiredo Jr 2007; D'Agostini et al. 2015). On tropical shelves, sedimentation exhibits spatially and temporally relationship with transgressive and regressive periods (Artusi and Figueiredo Jr 2007; D'Agostini et al. 2015). Particularly, in mixed systems, siliciclastic sediment deposition dominates during lowstand, while carbonatic production on shelves develops mainly during the transgressive and highstand periods. The sea-level fluctuations rule the accommodation space for sediment accumulation (e.g., Edwards et al. 2003), restrict the spatial distribution of coastal environments translating depocenters, and change the conditions involved in the carbonatic and siliciclastic sedimentation (e.g., D'Agostini et al. 2015). Besides, shallow strata have records of coastal and marine sedimentary processes of last sea-level cycle (Chaumillon

✉ D. A. Moreira
daniandrade.m@gmail.com

M. P. Gomes
gomesmp@geologia.ufrn.br

H. Vital
helenice@geologia.ufrn.br

[1] Post-Graduate Program in Geodynamics and Geophysics, Federal University of Rio Grande do Norte, Natal, Brazil

et al. 2008; Hinestrosa et al. 2014), which allow the regional reconstructions of Pleistocene and Holocene depositional systems and track sea-level changes.

High-resolution investigations on shallow strata of marine and transitional environments have revealed patterns and changes of depositional systems, including controls and conditions on fluvial incisions, wave and tide erosional processes, which are evident on infilling successions and key stratigraphic surfaces and structures (Gomes et al. 2016; D'Agostini et al. 2015; Edwards et al. 2003). The sequence boundary surface of the Pleistocene/Holocene has been worldwide associated with erosional surfaces formed during the Last Glacial Maximum (LGM), and higher-order surfaces with the interglacial Young Dryas period and the rise rate variations between meltwater pulses (Severinghaus et al. 1998; Bard et al. 2010; Abdul et al. 2016). Unconformities and the sequence boundary produced in the LGM were observed in Tahiti barrier reef at approximately 60 m below present sea level (Bard et al. 2010), similar to observed in reefs of Barbados (Peltier and Fairbanks 2006) and corals of the Huon Peninsula (Edwards et al. 1993; Cutler et al. 2003). After that, a maximum flooding surface observed over rapid transgression at 9800–9200 years BP correspondent a new MWP-1C with the sea-level rise from 36 to 16 m, diverted the Yellow River, modifying deposition. This diverted flow and rapid sea-level resulted in little or no sediment input (Liu et al. 2004).

In the northeastern Brazilian coast, the flooding initiated on Early Holocene and developed the backstepped carbonate reef system at outer shelves of Abrolhos shelf (D'Agostini et al. 2015) extending northward through the northern shelf of Rio Grande do Norte State (RN) (Nascimento Silva et al. 2018). Coastal retreat and estuarine development punctuated stages of sea-level rise at depths approximately 30 m before 9500 years BP and reached 22–28 m at 8200–9200 years BP and 6–11 m at 7800–8000 years BP on of mangrove sediments of the Potengi-Jundiaí Estuary (Kumar et al. 2018). Rapid inundation reached the modern sea level at 7000 years BP and its maximum at ~5000 years BP (highstand) at ~2–4 m above modern sea level followed by a gentle regressive trend up to the present-day sea level (Barbosa et al. 2018; Bezerra et al. 2003). The modern coast of Rio Grande do Norte (RN) (Fig. 1) has been strongly affected by erosion (Dominguez and Bittencourt 1996; Amaro et al. 2014; Vital et al. 2016). Although the influence of present-day sea-level rise is still in debate to this region, factors such as semiarid climate, low seaward contribution of eolian sediments, the lack of important rivers, high energy longshore transport, and widespread anthropic interference over the coastline might generate negative sediment balance and a starved shelf condition, which are responsible for the a scenario of regional coastal erosion on northeastern of Brazil (Pinheiro et al. 2016; Vital et al. 2010; Dominguez et al. 2016).

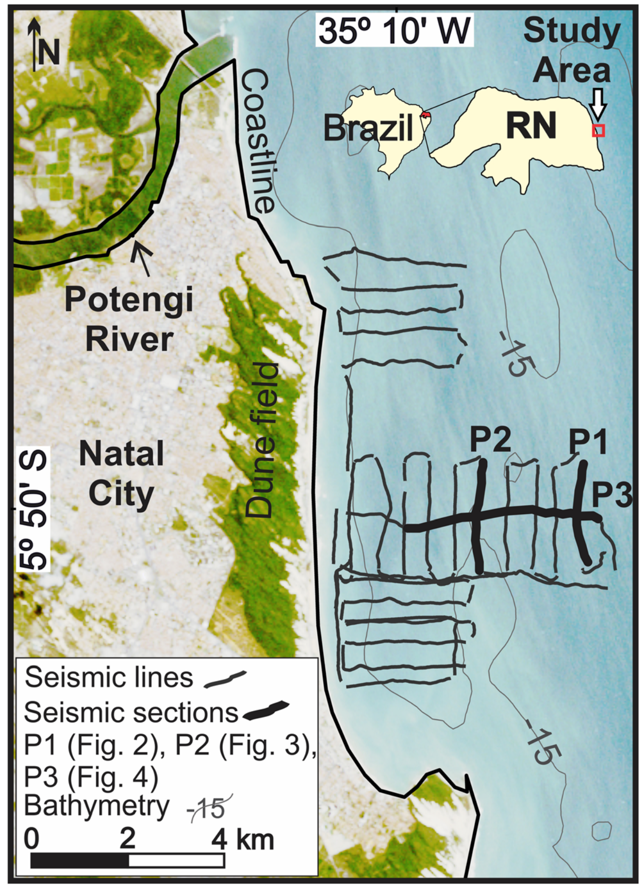

Fig. 1 Study area showing the location of seismic profiling lines. The P1, P2 and P3 seismic profiles represent the interpretation lines in Figs. 2, 3, and 4, respectively

It was investigated the shallow seismic architecture of Natal shelf, eastern of RN coast (Fig. 1), to reconstruct the depositional history since last postglacial transgression until present-day. Based on high-resolution seismic data, we track the effects of sea-level rise on sedimentary structures, which record factors that control the sedimentary balance during transgression, the magnitude of erosion and sedimentation, and the contrast of past and modern sedimentation.

Physical setting

The study area is located on the inner shelf of Natal, in the eastern of Rio Grande do Norte State (RN) (Fig. 1). This shelf is characterized by reduced depth, with shelf break at approximately 70-m water depth, and the maximum width of 40 km, and is dominated by mixed carbonate-siliciclastic sedimentation (Vital et al. 2008; Gomes et al. 2014). Interfingering of siliciclastic and carbonate sediments occurs since the Lower/Mid Miocene (Córdoba et al. 2007), and the modern shelf displays a well-defined trend of sediment mixing increasing carbonate offshore (Vital et al. 2010; Gomes et al. 2015). The coast region has outcrop sandstones of the Barreiras Formation, which forms continuous large cliffs along the coast, covered by Quaternary sediments such as dune fields along the coast, mangrove, alluvial and beach deposits (Mabesoone and Alheiros 1988). Cenozoic fault reactivations with a general NE trend shaped alternation of horsts and grabens on the cliffs and tectonic estuaries, conferring zeta curved bay geometry on the coast (Bezerra et al. 2001). The rivers are small and no significant contribution with the sedimentary input, generating a starved shelf condition (Vital et al. 2008). The main features of RN shelf are drowned beachrocks, found in depths of about 20 m, incised valleys, filled by Holocene sediments reaching a maximum thickness of 30 m, large sand ribbons, isolated sand bodies, and biogenic reefs attached to the coast and in the outer shelf (Vital et al. 2008, 2010; Gomes et al. 2014; Pereira et al. 2013; Nascimento Silva et al. 2018). In the study area, siliciclastic facies occur near the coast at depths of shallower than 8 m, with an increase of carbonate content to depths greater than 10 m (Oliveira 2017).

The region is dominated by mixed wave-tide conditions (Vital 2006), and the low gradient of the continental shelf contributes to the alongshore sediment transport (Amaro et al. 2014). Ribeiro et al. (2018) show currents in the region predominantly N direction, with higher intensities in the summer with 12.8 m/s, followed by spring with 9.3 m/s and autumn with 8 m/s. They can be modulated by the winds acting along the coast, and both tides and winds. The tides have a semidiurnal mesotidal regime with a tidal range between 0.85 and 2.30 m (Hayes 1979; Frazão 2003). The nearshore wave patterns were determined by the variations of the trade winds. Their height increases toward the north reaching 2.5 m in storm conditions ENE while in south region maximum values reached 1.5 m in storm conditions and 1 m in median conditions (Almeida et al. 2015). The pattern of the trade winds in the region presents strong SE trend (Barros et al. 2013; Ribeiro et al. 2018), varying seasonally between SSE and ESE, with velocities of 3.8 to 5 m/s and coastal drift that transports sediments in the S-N direction (Vital 2006).

Materials and methods

High-resolution seismic data were acquired in August 2015, covering an area of 30 km^2 with 62 km of lines distributed in 17 longitudinal profiles (N-S) and 14 perpendiculars (E-W) to the coastline, with space between profiles of 0.5 km (Fig. 1). These profiles were collected onboard a medium-sized vessel with a Meridata Boomer System operating with 50 J of energy, frequencies ranging from 1 to 2 kHz associated with a single-channel streamer with 8 hydrophones. The data were acquired with Meridata MDCS software and converted to SEG-Y. Navigation was acquired using a Hemisphere V100 model DGPS system. The seismic data were processed in ReflexWin, Oasis Montaj, and SeiSee auxiliary software. The processing flow consisted of predictive deconvolution, static correction, bandpass frequency, AGC gain, and average filters (e.g., Gomes et al. 2014, 2016). After processing, the vertical resolution of the data was 0.5 cm. Two-way travel time was converted into depth in meters (m) assuming the speed of sound 1500 m/s (e.g., Quinn et al. 1998; Lericolais et al. 1990; Gomes et al. 2016). The seismic stratigraphic interpretations were based on reflector continuity, amplitude, lateral extension, morphology, configuration (parallel, wavy, chaotic), and terminations (onlap, downlap, offlap, and truncations) (Van Wagoner et al. 1988; Mitchum et al. 1977). The main reflectors were mapped and used to generate geomorphic surfaces, using software Petrel in time (ms). The mapping of seismic facies and reflector geometry allowed the interpretation of the paleoenvironment associated with the seismic units.

Results

Three most prominent surfaces (S1–S3) and seismic units (U1–U3) with distinctive acoustic characters were identified in the inner shelf of Natal (Figs. 2, 3, and 4). Seismic units were described in terms of seismic facies and their environmental context (Table 1). All units and surfaces were identified in the whole area except surface S1 and U1.

Surface S1 is a regional, irregular, and discontinuous surface with high amplitude on the central and north study area. Its irregular morphology on a large scale promotes rugged relief with steep slopes (Figs. 2, 3, and 4). S1 is the base of U1 and an erosional truncation on U1 is generally observed about 10 ms (~ 13 m). This surface reaches depths in central region landward with ~ 44 ms (~ 34 m) and 52 ms (~ 43 m) locally (Fig. 5d). The S1 becomes shallower toward the northeast.

Unit U1 is the lowest unit described, laying on S1 and limited above by S2. This unit occurs at 20–30 ms (16–25 m) with a greater thickness (25 m) in the central area and shallower northward. This unit is not clear in the south region due to acoustic turbidity. U1 has a lateral variation of facies with chaotic and parallel patterns. The chaotic configuration reflects a disordered internal organization of the deposition that suggests a variable energy source and intensity of depositional environment or deformations (illustration II in Table 1). The parallel reflectors are discontinuous with low frequencies and alternating moderate to low amplitudes reflections. Onlap terminations are present on S1 while the top of this unit is concordant with S2.

Surface S2 is a regional, irregular, and moderate continuity surface. It limits units U1 and U2 and reached ~ 32 ms (22 m) near the coast, where the deepest occurrence is, and ~ 26 ms (18 m) in other regions (Fig. 5c). The S2 occurs at shallower depths southward. Several channel-like morphology shapes

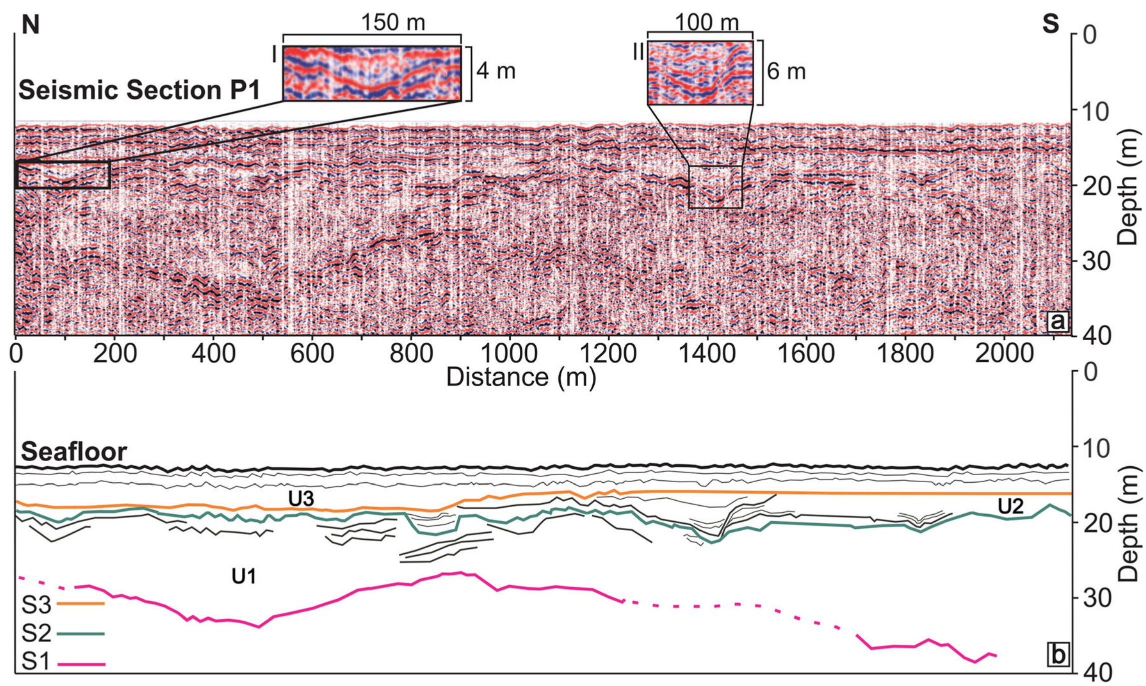

Fig. 2 Boomer seismic profile (P1 in Fig. 1) parallel and more distal to the coast (**a**) and interpretation (**b**). (I) channel-like morphology dimensions of S2; (II) channel-like morphology with erosional truncation and dimensions of S2

this horizon in variable sizes with widths ~ 100–200 m and depths of ~ 4–10 m NS (Figs. 2-I-II, 3-II) and ~ 240–323 m and depths of ~ 7–10 m EW (Fig. 4-I-II) indicating a possible wave-tide ravinement surface. In general, all channels have different shapes since symmetric (Fig. 2-I; Fig. 4-I-II), asymmetric (Fig. 3-II) to steep (Fig. 3-I). These features are more prominent in the central region (Fig. 5c). The moderate continuity and the irregular geometry of S2 suggest that different

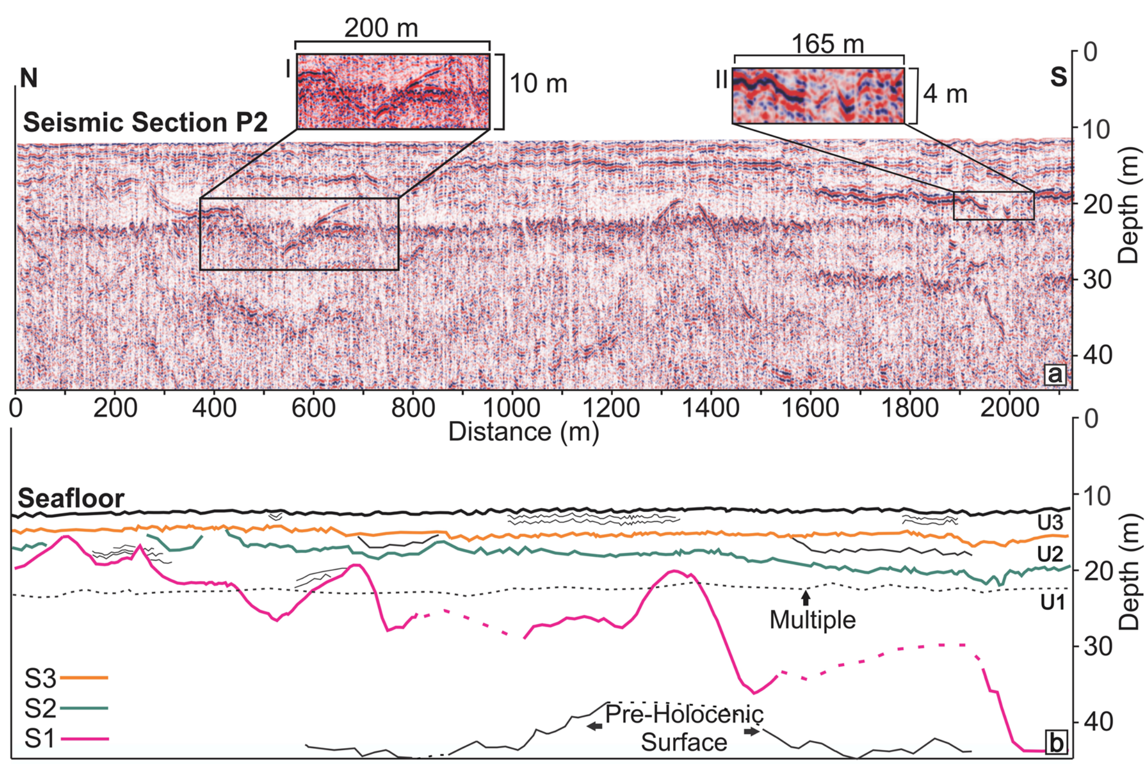

Fig. 3 Boomer seismic profile (P2 in Fig. 1) parallel the coast (**a**) and interpretation (**b**). (I) prominent relief with a steep slope of surface S1; (II) irregular channel-like morphology of S2

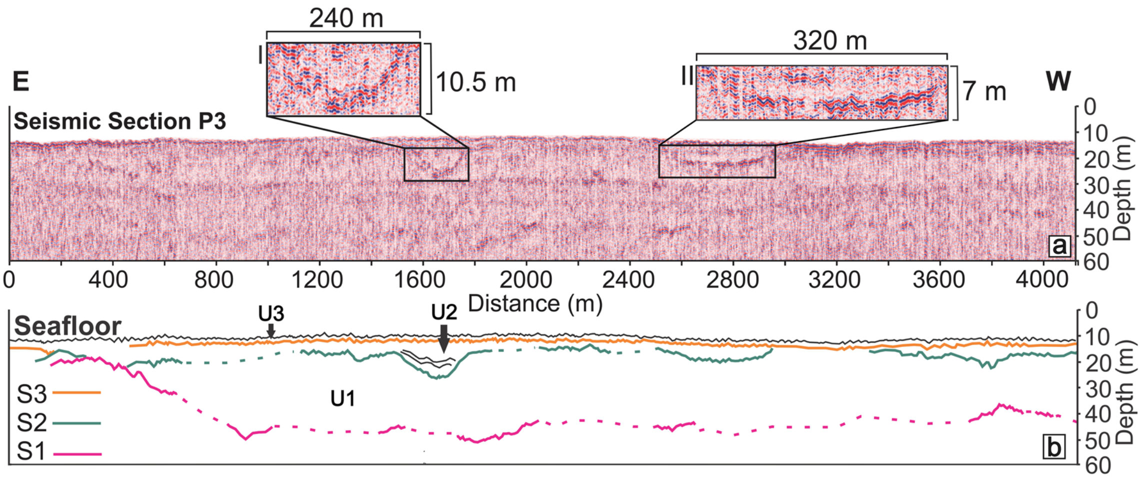

Fig. 4 Boomer seismic profile (P3 in Fig. 1) perpendicular to the coast (**a**) and interpretation (**b**). (I) and (II) symmetric relief of S2 and dimensions

erosional and sedimentation processes acted regionally along the whole area.

Unit U2 is an intermediate unit limited by S2 and S3. This unit occurs in the whole study area at depths of 10 ms (8.3 m) with thickness up to 7 ms (6 m) southward. U2 has moderate frequency and alternating moderate to low amplitude reflections that indicate low contrast of sediments. Locally reflections are continuous, with moderate amplitudes and low frequencies. Onlap terminations are evident on S2 and erosional truncate on top in S3 (Fig. 2-II). This unit fills the channel-like feature and might represent transgressive deposits filling the ravinement surface.

Surface S3 is regular with high continuity and amplitude surface occurring in the entire study area at depths of about ~ 20 ms (14 m) (Fig. 5b). S3 is nearly parallel beneath the seafloor reflection and coincides locally with S2 (Figs. 2 and 3). This is a parallel/wavy surface that limits U2 and U3 in conformity reflections.

Unit U3 is the younger unit, laying on S3, and is bounded on top by seafloor reflector. Parallel to wavy reflections with high continuity and amplitude and low frequency is observed in the whole study area. Parallel configuration indicates uniform sedimentation while high amplitudes indicate vertical sediment alternation depicting an aggradational deposition pattern. This is well-bedded marine sediments marked by low frequency. High continuity characterizes similar sedimentation conditions in large lateral extension. The low frequency and high amplitude deposits may be due to coarse material, probably biogenic as observed on the seafloor surface. U3 has a thickness of 4–6 ms (3–5 m) thinning 2 ms (1.5 m) southward.

The seafloor has smooth relief with wavy morphology that follows U3 deposition (Figs. 2, 3, and 4). It is deeper seaward at ~ 17 ms (~ 12 m) and toward the northern reaches at ~ 20 ms (~ 14 m), and shallower in the south region and near the coast at ~ 14 ms (10 m) (Fig. 5).

The sediment volume and thickness of the units were calculated by the difference between consecutive surfaces (Fig. 6). The lowest unit U1 (the difference between S1 and S2) (Fig. 6a) shows major variability of thickness spatially along the area, especially in the central region with 16 ms

Table 1 Characteristics of acoustic facies and seismic units, and the interpretation in terms of depositional environment. Illustrations: (I) parallel/wavy reflectors; (II) onlapping reflections on S2; (III) channel infilling; (IV) truncation on S3; (V) parallel reflectors; (VI) chaotic reflectors; (VII) onlapping reflections on S1

Sea-level condition	Seismic units	Character	Seismic facies	Illustration	Sedimentation and environments
HST	U3	High continuity low frequency high amplitude	Parallel/wavy configuration with concordant reflectors and without terminations	I 	• Low energy shallow marine environment • Aggrading
	MF—S3				
Mid- to High TST	U2	High continuity moderate frequency and moderate to low amplitude	Reflectors onlapping or concording infilling valleys in S2 on basis and truncates S3 on top	II 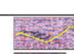 III 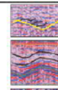 IV 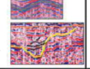	• Uniform energy environment • Shallow marine - closure of semi confined environment
	TR²—S2				
Lower TST	U1	Low continuity and frequency variable amplitude	Parallel to chaotic reflectors onlapping S2 and S1 and concordant reflectors above S1	V 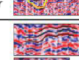 VI 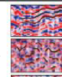 VII 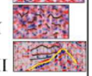	• High- to moderate-energy • Shallow marine with semi confined environment
	TR¹ S1				

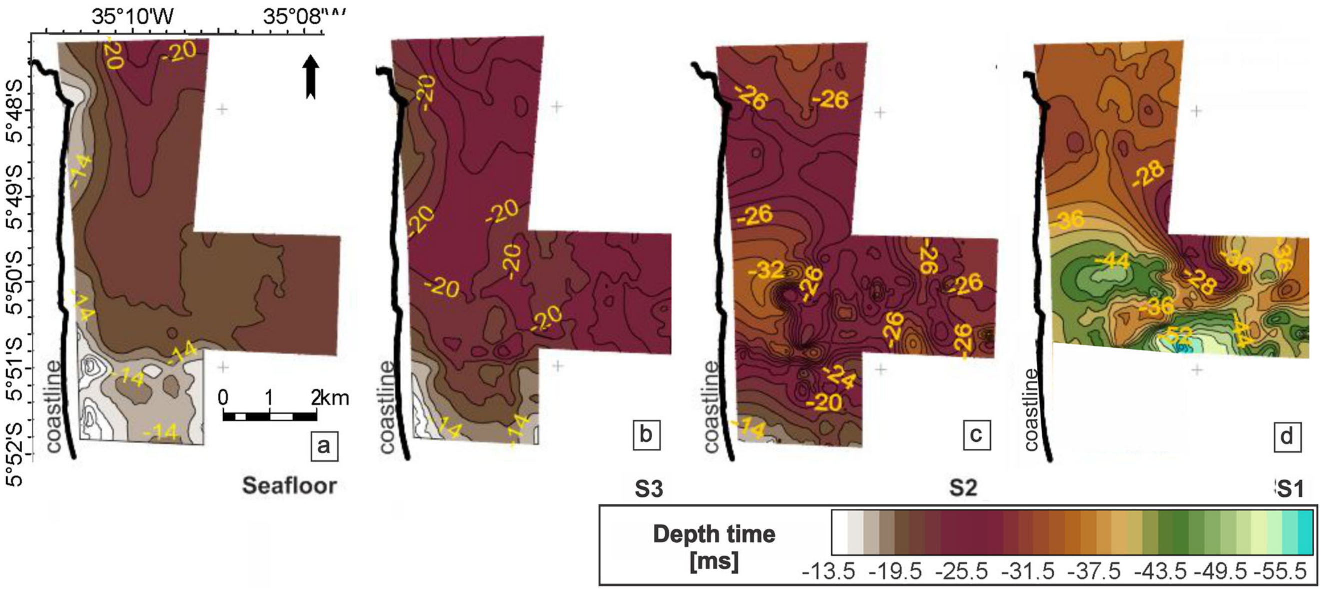

Fig. 5 The 2D surface maps of the seafloor (**a**), S3 (**b**), S2 (**c**), and S1 (**d**). The colors represent depth time (ms)

(~ 12 m) of thickness. In the north region, the difference is smaller with 8 ms (~ 6 m) thick. Into the intermediate unit U2, the difference between S2 and S3 (Fig. 6b) is smaller. In central region, sediment thickness reached 4 ms (~ 3 m) seaward predominantly and near the coast reached 12 ms (~ 9 m) thick. In other regions, 4 ms (~ 3 m) of sediment thickness prevails. A little variability of U3 thickness (Fig. 6c) exhibits an average of 4 ms (~ 3 m) of thickness in most of the study area. At seaward, this thickness increases at 8–10 ms (~ 6–7.5 m). In general, near the coast at central region experienced major sediment thickness in the oldest unit U1 while the thickness of U2 and U3 decrease in the whole area.

Discussions and conclusions

The last marine regression and transgression on Natal shelf left stratigraphic marks of interactions between the shelf and coastal processes. The S1 is a prominent and very irregular surface (deepest scours at ~ 40 m and mound-like feature at ~ 20 m) which delineates the top of the acoustic basement (no signal penetration) (S1 in Figs. 2, 3, and 4). According to the sea-level position on far-field curves (Severinghaus et al. 1998; Bard et al. 2010; Abdul et al. 2016), the S1 occurrence pattern suggests that this surface was formed in a shelf exposure, or transgressive ravinement, and might represent a regional unconformity between Pleistocene and Holocene. Coastal parabolic dunes, over sandstone cliffs, in the study area (~ 83,000 years BP) (Julio 2018), SE-NW oriented due to the southeasterly wind flow, serve as evidence that the exposed shelf in the southeast was probably the sediment source. Moreover, rework of these siliciclastic sediments might be the formed the initial transgressive deposits. This surface might be related to the top of the Pleistocene rocks of Barreiras Formation, which outcrops locally in the near coastline as well as widespread cliffs along RN coast (Vital et al. 2016). This rocky formation was largely eroded creating the boundary surface, but locally reactivated during transgression by wave-tide ravinement (see S2 in Figs. 3 and 4). Besides, near the present-day coastline, the S1 becomes deeper forming a depression morphology (Fig. 5). This may be associated with a long-term nearshore erosion process associated with a cliff rocky coast, which provides a low rate of coastline migration landward during the Holocene (Vital et al. 2006, 2016).

Parallel to the chaotic internal configuration of U1 lying above S1 suggests moderate to high-energy regimes of very shallow marine or the nearshore environment. The sediment dynamics of this shallow marine portion was probably controlled by the wave-tide regimes and the early establishment of southerly alongshore currents (Ribeiro et al. 2018). The depths of the occurrence of U1 indicate that the shelf inundation and deposition system started at the end of MWP-1B (Severinghaus et al. 1998). The depth increasing of S1 near coastline provided a semi-confined depression morphology in the center of the study area. And the smoothed top surface (S2) revealed a considerable accommodation space and sediment budget during the early shelf inundation as occurring in transgressive systems as embayment, estuaries, and incised valleys in the Bay of Biscay (Lericolais et al. 2001; Chaumillion et al. 2008; Green et al. 2015).

The ravinement surface S2 clearly displays non-continuous scours occurring in higher depths near the coast (S2 in Figs. 2, 3, and 4). This erosional surface has been interpreted as typically transgressive surface in estuarine

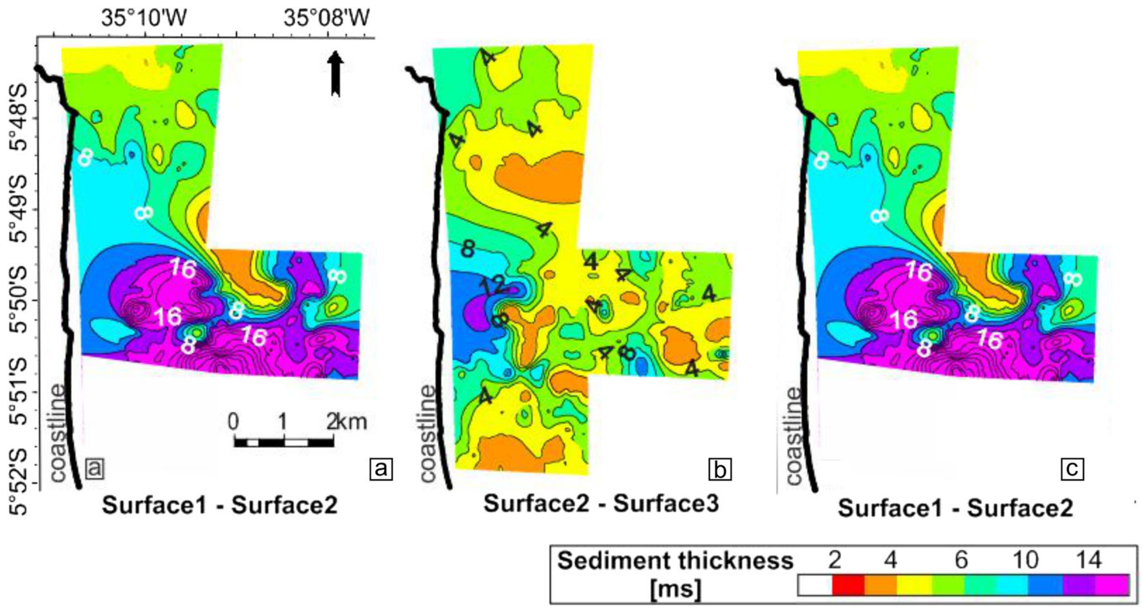

Fig. 6 Maps of sediment volume between S3-seafloor being the unit U3 (**a**), S2-S3 being the unit U2 (**b**), and S1-S2 being the unit U1 (**c**). The colors represent the relative sediment thickness (ms)

successions (Lericolais et al. 2001; Chaumillion et al. 2008; Catuneanu et al. 2011), which indicate the wave-tide action controlling the sediment dynamics (Zeiler et al. 2008) in a shallow shelf environment under significant reworking of sediments (Lericolais et al. 2001; Chaumillion et al. 2008). The S2 occurs at ~ 18 m below modern sea level, and this depth has probable relation with sea-level rise deceleration (Severinghaus et al. 1998).

The depositional changes observed in U2 and U3, with parallel/wavy reflectors, featureless, and smooth morphology on top (S3) following the seabed morphology, reflect a decrease of energy associated with an increase of water depth. This pattern punctuates the end of coastline-connected sedimentation, with the initial infill of the channel-like ravinement features observed on S2, and a subsequent establishment of aggradation pattern that was probably dominated by carbonate as observed in the present seafloor (Oliveira 2017). The absence of truncation of reflector terminations on top S3 evidences the maximum flooding. This is a synchronous event caused by rapid sea-level rise and complete shelf inundation (Aleman et al. 2014; Menier et al. 2010; Lericolais et al. 2001; Hinestrosa et al. 2014; Gomes et al. 2016; D'Agostini et al. 2015). Additionally, the smaller thickness of U2 and U3 reveals lower rates of accumulation, which might be associated with lower sediment supply and aggradation common of carbonate deposits (Gomes et al. 2015), and yet low water depth controlling the accommodation space (Veeken and Moerkerken 2013).

The stratigraphic succession of the inner shelf of Natal reveals that the siliciclastic sediment accumulation (or supply) has decreased along the Holocene (Fig. 6) with the increase of water depth and carbonate content. This may corroborate to explain why the modern seafloor of Natal Shelf has depths of approximately 15 m very close to the coastline (at ~ 1 km). In comparison, this depth of 15 m occurs far from the coast (~ 30 km) in the RN shelves on the north (e.g., Touros, Macau, Gomes et al. 2014; Testa and Bosence 1998). These shelves on north have larger inner shelves and are dominated by siliciclastics and dissipative beaches, and the large parabolic dune fields spread on the adjacent coasts (Testa and Bosence 1998; Gomes et al. 2014), while Natal Shelf has a narrow tongue of siliciclastics sediments attached to coastline, reflective beaches, active cliffs, and smaller dune fields (Vital et al. 2016). However, the oceanography and climate regimes are nearly the same during Holocene until present-day to the whole RN shelf (Dominguez et al. 1992), including the alongshore sediment transport and erosion (Vital et al. 2006, 2016; Vital 2006). Additionally, coastline migration landward in the Natal coast should be minimal in comparison with the north coast of RN, due to the cliff coast settings. Therefore, the main factor controlling the coastal sediment balance is the local contexts associated with the geomorphological heritage and the potential of preservation under high energy oceanographic regimes able to accumulate large active subaqueous dunes of siliciclastic sediments on northern shelves (Gomes et al. 2014) while the Natal Shelf is starved.

Acknowledgments Thanks are due to the Luiz A. P. Souza, Moysés G. Tessler, the TETRATEC and the GGEMMA group for their survey support, as well as PPGG/UFRN for the academic and scientific infrastructure. This is a contribution of INCT AmbTropic – Brazilian National Institute of Science and Technology for Tropical Marine Environments 565054/2010-4, 8936/2011 & 465634/ 2014-1 (CNPq/FAPESB/ CAPES). We are grateful for Schlumberger by Petrel E&P software.

Funding information Funds for this research were provided by the PRH-229-PETROBRAS for funding the master's scholarship of the first author, and CNPq for a Research Fellowship (grant PQ 311413/2016-1) to the third author, and the projects: Ciências do Mar II 23038.004320/2014-11 (CAPES), IODP 88887.123925/2015-00 (CAPES).

References

Abdul NA, Mortlock RA, Wright JD, Fairbanks RG (2016) Younger Dryas sea level and meltwater pulse 1B recorded in Barbados reef crest coral Acroporapalmata. Paleoceanogr 31:330–344

Aleman N, Certain R, Barusseau JP, Courp T, Dia A (2014) Post-glacial filling of a semi-enclosed basin: the Airgun Basin (Mauritania). Mar Geol 49:126–135

Aliotta S, Ginsberg SS, Spagnuolo JO, Farinati E, Giagante D, Vecchi LG (2013) Late Quaternary in a South Atlantic estuarine system: stratigraphic and paleontologic indicators of coastal evolution. J S Am Earth Sci 45:194–208

Almeida LR, Amaro VE, Marcelino AMT, Scudelari AC (2015) Avaliação do clima de ondas da praia de Ponta Negra (RN, Brasil) através do uso do SMC-Brasil e sua contribuição à gestão costeira. J Integr Coast Zone Manag 15(2):135–151

Amaro VE, Gomes LRS, Lima FGF, Scudelari AC, Neves CF, Busman DV, Santos ALS (2014) Multitemporal analysis of coastal erosion based on multisource satellite images, Ponta Negra Beach, Natal City, northeastern Brazil. Mar Geod 38:1–25

Artusi L, Figueiredo AG Jr (2007) Sismoestratigrafia Rasa da Plataforma Continental de Cabo Frio – Araruama – RJ. Ver Bras Geofís 25(1): 7–16

Barbosa MEF, Boski T, Bezerra FHR, Lima-Filho FP, Gomes MP, Pereira LC, Maia RP (2018) Late Quaternary infilling of the Assu River embayment and related sea level changes in NE Brazil. MarGeol 405:23–37

Bard E, Hamelin B, Delanghe-Sabatier D (2010) Deglacial meltwater pulse 1B and Younger Dryas sea levels revisited with boreholes at Tahiti. Science 327:1235–1237

Barros J D, Furtado M L S, Costa A M B, Marinho G S, Silva F M (2013) Sazonalidade do vento na cidade de Natal/RN pela distribuição de Weibull. Rev Sociedade e Território Natal 25(2) EE: 78-92

Benallack K, Green AN, Humphries MS, Cooper JAG, Dladla NN, Finch JM (2016) The stratigraphic evolution of a large back-barrier lagoon system with a non-migrating barrier. Mar Geol 379:64–77

Bezerra HR, Amaro VE, Vita-Finzi C, Saadi A (2001) Pliocene-Quaternary fault control of sedimentation and coastal plain morphology in NE Brazil. J S Am Earth Sci 14(1):61–75

Bezerra FHR, Barreto AMF, Suguio K (2003) Holocene sea-level history on the Rio Grande do Norte State Coast, Brazil. Mar Geol 196:73–89

Bird MI, Austin WEN, Wurster CM, Fifield K, Mojtahid M, Sargeant C (2010) Punctuated eustatic sea-level rise in the early mid-Holocene. Geology 38(9):803–806

Caldas LHO, Stattegger K, Vital H (2006) Holocene sea-level history: evidence from coastal sediments of the northern Rio Grande do Norte coast, NE Brazil. Mar Geol 228:39–53

Campos RHS, Dominguez JML (2010) Mobility of sediments due to wave action on the continental shelf of the northern coast of the state of Bahia. Braz J Oceanogr 58(2):57–63

Catuneanu O, Galloway WE, Kendall CGSC, Miall AD, Posamentier HW, Strasser A, Tucker M (2011) Sequence stratigraphy: methodology and nomenclature. Newsl Stratigr 44(3):173–245

Chaumillon E, Proust J, Menier D, Weber N (2008) Incised-valley morphologies and sedimentary-fills within the inner shelf of the Bay of Biscay (France): a synthesis. J Mar Syst 72:383–396

Cooper JAG, Meireles RP, Green AN, Klein AHF, Toldo EE (2018) Late Quaternary stratigraphic evolution of the inner continental shelf in response to sea-level change, Santa Catarina, Brazil. Mar Geol 397: 1–14

Córdoba VC, Jardim de Sá EF, Souza DC, Antunes FA (2007) Bacia Pernambuco-Paraíba. BGeociPetrobrás, Rio de Janeiro 15(2):391–403

Cutler KB, Edwards RL, Taylor FW, Cheng H, Adkins J, Gallup CD, Cutler PM, Burr GS, Bloom AL (2003) Rapid sea-level fall and deep-ocean temperature change since the last interglacial period. Earth Planet Sci Lett 206:253–271

D'Agostini DP, Bastos AC, Reis AT (2015) The modern mixed carbonate-siliciclastic Abrolhos Shelf: implications for a mixed depositional model. J Sediment Res 85:124–139

Dominguez JML, Bittencourt ACSP (1996) Regional assessment of long-term trends of coastal erosion in northeastern Brazil. An Acad Bras Cienc 68:355–372

Dominguez JML, Bittencourt ACSP, Martin L (1992) Controls on Quaternary coastal evolution of the east-northeastern coast of Brazil: roles of sea-level history, trade winds and climate. Sediment Geol 80:213–232

Dominguez JML, Neves SM, Bittencourt ACSP (2016) Sandy beaches of the state of Paraíba: the importance of geological heritage. In: Andrew D. Short; Antonio Henrique da F. Klein. (Org.). Brazilian beach systems. 1st ed. Springer International Publishing, Switzerland, pp 231–229

Edwards RL, Beck JW, Burr GS, Donahue DJ, Chappell JM, Bloom AL, Druffel ER, Taylor FW (1993) A large drop in atmospheric 14C/12C and reduced melting in the Younger Dryas, documented with 230ThAges of corals. Science 206(5110):962–968

Edwards JH, Harrison SE, Locker SD, Hine AC, Twichell DC (2003) Stratigraphic framework of sediment-starved sand ridges on a mixed siliciclastic/carbonate inner shelf: west-central Florida. Mar Geol 200:195–217

Frazão EP (2003) Caracterização hidrodinâmica e morfo-sedimentar do estuário Potengi e áreas adjacentes: subsídios Pará controles e recuperação ambiental no caso de derrames de hidrocarboneto. Dissertation, Universidade Federal do Rio Grande do Norte

Gomes MP, Vital H, Bezerra FHR, Castro DL, Macedo JWP (2014) The interplay between structural inheritance and morphology in the equatorial continental shelf of Brazil. Mar Geol 355:150–161

Gomes MP, Vital H, Eichler PPB, Gupta BKS (2015) The investigation of a mixed carbonate-siliciclastic shelf, NE Brazil: side-scan sonar imagery, underwater photography, and surface-sediment data. Ital J Geosci 134(1):9–22

Gomes MP, Vital H, Stattegger K, Schwarzer K (2016) Bedrock control on the Assu Incised Valley morphology and sedimentation in the Brazilian equatorial shelf. Int J Sediment Res 31:181–193

Green AN, Cooper JA, Wiles EA, Lecea AM (2015) Seismic architecture, stratigraphy and evolution of a subtropical marine embayment: Maputo Bay, Mozambique. Mar Geol 369:300–309

Hayes MO (1979) Barrier Island morphology as a function of tidal and wave regime. In: Leatherman SP (ed) Barrier Islands from the Gulf of St. Lawrence to the Gulf of Mexico. Academic Press, New York, pp 1–27

Hinestrosa G, Webster JM, Beaman RJ, Anderson LM (2014) Seismic stratigraphy and development of the shelf-edge reefs of the Great Barrier Reef, Australia. Mar Geol 353:1–20

Julio K (2018) Caracterização, modelagem, origem e evolução dos depósitos Pós- Barreiras e sistemas eólicos em Pitangui, RN. Thesis, Universidade Federal do Rio Grande do Norte

Kalani M, Khodabakhsh S, Amirbehboudi C (2008) Seismic expression and inferred depositional environments of Plio-Pleistocene sedimentary sequences in the southwestern Caspian Sea. Geo-Mar Lett 28: 31–41

Kumar M, Boski T, Lima-Filho FP, Bezerra FHR, González-Vila FJ, González-Pérez JA (2018) Environmental changesrecorded in theHolocene sedimentar infill of a tropical estuary. QuaternInt 476: 34–45

Lambeck K, Rouby H, Purcell A, Sun Y, Sambridge M (2014) Sea level and global ice volumes from the Last Glacial Maximum to the Holocene. Proc Natl A Sci 111(43):15296–15303

Lericolais G, Allenou JP, Morvan P (1990) A new system for acquisition and processing of very high-resolution seismic reflection data. Geophysics 55(8):1036–1046

Lericolais G, Berné S, Féniès H (2001) Seaward pinching out and internal stratigraphy of the Gironde incised valley on the shelf (Bay of Biscay). Mar Geol 175:183–197

Liu JP, Milliman JD, Gao S, Cheng P (2004) Holocene development of the Yellow River's subaqueous delta, North Yellow Sea. Mar Geol 209:45–67

Mabesoone JM, Alheiros MM (1988) Origem da Bacia sedimentar costeira Pernambuco-Paraíba. Rev Bras Geoc 18(4):476–482

Menier D, Tessier B, Proust J, Baltzer SP, Traini C (2010) The Holocene transgression as recorded by incised-valley infilling in a rocky coast context with low sediment supply (southern Brittany, western France). Bull Soc Géol Fr 81(2):115–128

Mitchum R M, Vail P R, Thompson S (1977) Seismic stratigraphy and global changes of sea level, part 2: the depositional sequence as a basic unit for stratigraphic analysis

Muehe D (2010) Brazilian coastal vulnerability to climate change. Pan-Am J Aquat Sci 5(2):173–183

Nascimento Silva LL, Gomes MP, Vital H (2018) The Açu Reef morphology, distribution and inter reef sedimentation on the outer shelf of the NE Brazil equatorial margin. Cont Shelf Res 160:10–22

Nittrouer CA, Austin JA, Field ME, Kravitz JH, Syvitski JPM, Wiberg PL, editors (2007) Continental margin sedimentation: from sediment transport to sequence stratigraphy. Malden: Blackwell Publishing. Int AsSed 37

Oliveira CA (2017) Heterogeneidade espacial do substrato plataformal adjacente a Ponta Negra, Natal, RN. Dissertation, Universidade Federal do Rio Grande do Norte

Peltier WR (1998) Global glacial isostatic adjustment and coastal tectonics. In: Stewart I, Vita-Finzi C (Eds) CoastalTectonics- Geol. Soc. London Special Publ 146, pp 1–29

Peltier WR, Fairbanks RG (2006) Global glacial ice volume and Last Glacial Maximum duration from an extended Barbados sea-level record. Quat Sci Rev 25:3322–3337

Pereira TRB, Vital H, Silva JPF (2013) Aplicação da Batimetria Multifeixe para análise da morfologia do fundo marinho adjacente a praia de Ponta Negra – RN. 13th Int Congress Braz Geophys Soc

Pinheiro LS, Morais JO, Maia LP (2016) The beaches of Ceará. In: Andrew D. Short; Antonio Henrique da F. Klein. (Org.). Brazilian beach systems. 1st ed. Springer International Publishing, Switzerland, pp 175-199

Quinn R, Bull JM, Dix JK (1998) Optimal processing of marine high-resolution seismic reflection (Chirp) data. Mar Geophys Res 20:13–20

Ribeiro F, Pimenta FM, Vital H (2018) Inner shelf currents of Ponta Negra beach, Natal, RN, Brazil. Rev Bras Geofís 36(1):43–58

Severinghaus JP, Sowers T, Brook EJ, Alley RB, Bender ML (1998) Timing of abrupt climate change at the end of the Younger Dryas interval from thermally fractionated gases in polar ice. Nature 391: 141–146

Tesson M, Posamentier H, Gensous B (2015) Compound incised-valley characterization by high-resolution seismics in a wave-dominated setting: example of the Aude and Orb rivers, Languedoc inner shelf, Gulf of Lion, France. Mar Geol 367:1–21

Testa V, Bosence DWJ (1998) Carbonate-siliciclastic sedimentation on a high-energy, ocean-facing, tropical ramp, NE Brazil. In: Wright VP, Burchette TP (eds) Carbonate ramps. Geological Society, London, Special Publications, 149, pp 55–71

Van Wagoner JC, Posamentier HW, Mitchum RM, Vail PR, Sarg JF, Loutit TS, Hardenbol J (1988) An overview of the fundamentals of sequence stratigraphy and key definitions. In Wilgus C K, Posamentier H W, Ross C K, Kendall C G St C, eds., Sea-level changes: an integrated approach: Tulsa, SEPM Spec P 42: 39–45

Veeken PCH, Moerkerken B (2013) Seismic stratigraphy and depositional facies models. EAGE Publications

Vital H (2006) Erosão e progradação no litoral do Rio Grande do Norte. In: Muehe D. Erosão e progradação do litoral brasileiro. Brasilia, DF: Ministério do MeioAmbiente, pp 159-176

Vital H, Amaro VE, Silveira IM (2006) Coastal erosion on the Rio Grande do Norte State (northeastern Brazil): causes and factors versus effects and associated processes. J Coast Res SI 39:1307–1310

Vital H, Statteger K, Amaro VE, Schwarzer K, Frazão EP, Tabosa W, Silveira IM (2008) A modern high-energy siliciclastic-carbonate plataforma: continental shelf adjacente to northern Rio Grande do Norte state, Northeastern Brazil. J Sediment Res 90:175–188

Vital H, Gomes MP, Tabosa WF, Frazão EP, Santos CLA, Plácido Junior JS (2010) Characterization of the Brazilian continental shelf adjacent to Rio Grande do Norte State, NE Brazil. Braz J Oceanogr 58(spec issue, IGCP526):43-54

Vital H, Silveira IM, Tabosa WF, Lima ZM, Lima Filho FP, Souza FES, Chaves MS, Pimenta FM, Gomes MP (2016) Beaches of Rio Grande do Norte. In: Andrew D. Short; Antonio Henrique da F. Klein. (Org.). Brazilian beach systems. 1st edn. Springer International Publishing, Switzerland pp 201-229

Zeiler M, Schwarzer K, Bartholomä A, Ricklefs K (2008) Seabed morphology and sediment dynamics. Die Küste 74:31–44